INTERNATIONAL JOURNAL OF
NUMERICAL ANALYSIS AND MODELING
Volume 12, Number 1, Pages 54–80

STABILITY OF THE KINEMATICALLY COUPLED β-SCHEME FOR FLUID-STRUCTURE INTERACTION PROBLEMS IN HEMODYNAMICS

SUNČICA ČANIĆ, BORIS MUHA, AND MARTINA BUKAČ

(Communicated by Max Gunzburger)

Abstract. It is well-known that classical Dirichlet-Neumann loosely coupled partitioned schemes for fluid-structure interaction (FSI) problems are unconditionally unstable for certain combinations of physical and geometric parameters that are relevant in hemodynamics. It was shown in [18] on a simple test problem, that these instabilities are associated with the so called "added-mass effect". By considering the same test problem as in [18], the present work shows that a novel, partitioned, loosely coupled scheme, recently introduced in [11], called the kinematically coupled β-scheme, does not suffer from the added mass effect for any $\beta \in [0, 1]$, and is unconditionally stable for all the parameters in the problem. Numerical results showing unconditional stability are presented for a full, nonlinearly coupled benchmark FSI problem, first considered in [31].

Key words. Fluid-structure interaction, Partitioned schemes, Stability analysis, Added-mass effect

1. Introduction

Fluid-structure interaction (FSI) problems have important applications in various areas including bio-fluids and aero-elasticity. They have been extensively studied from the numerical, as well as analytical point of view [5, 7, 8, 9, 10, 19, 20, 21, 23, 24, 28, 30, 32, 36, 38, 39, 41, 42, 48, 49, 50, 55, 56]. A set of popular numerical schemes for FSI in blood flow includes partitioned schemes (loosely or strongly coupled). Partitioned schemes typically solve an underlying multi-physics problem by splitting the problem into sub-problems determined by the different physics in the coupled problem. In particular, in fluid-structure interaction problems the fluid dynamics and structure elastodynamics are often solved using separate solvers. In loosely coupled schemes only one iteration between the fluid and structure subproblem is performed at each time step, while in strongly coupled schemes several sub-iterations between the fluid and structure sub-problems need to be performed at each time step to achieve stability.

The main advantages of *loosely coupled partitioned schemes* are modularity, simple implementation, and low computational costs. However, in [18] it was proved that for certain combinations of physical and geometric parameters (which are realistic in blood flow) "classical" Dirichlet-Neumann loosely coupled schemes are unconditionally unstable. In the same paper, the authors showed that this instability is due to the "added-mass effect". Namely, it was shown that a portion of the fluid load to the structure in the coupled FSI problems can be written as an additional inertia term in the structure equation coming from the fluid mass (added mass). In numerical schemes in which this term appears *explicitly*, which is the case in the classical Dirichlet-Neumann loosely coupled partitioned schemes, the

Received by the editors May 10, 2013 and, in revised form, April 23, 2014.
2000 *Mathematics Subject Classification.* 35R35, 49J40, 60G40.
Corresponding author: Sunčica Čanić.

added mass term acts as a source of instabilities when the structure is too "light" to counter-balance the kinetic energy of the "heavy" fluid load.

To get around these difficulties, several different loosely coupled algorithms have been proposed. The method proposed in [5] uses a simple membrane model for the structure which can be easily embedded into the fluid problem where it appears as a generalized Robin boundary condition. In this way the original problem reduces to a sequence of fluid problems with a generalized Robin boundary condition which can be solved using only the fluid solver. A similar approach was proposed in [48] where the fluid and structure were split in the classical way, but the fluid and structure sub-problems were linked via novel transmission (coupling) conditions that improve the convergence rate. A different approach to stabilization of loosely coupled (explicit) schemes was proposed in [16] based on the Nitsche's method [35]. We further mention the scheme proposed in [6] where a Robin-Robin type preconditioner was combined with Krylov iterations for a solution of an interface system.

For completeness, we also mention several semi-implicit FSI schemes. The schemes proposed in [27, 1, 2] separate the computation of fluid velocity from the coupled pressure-structure velocity system, thereby reducing the computational costs. Similar schemes, derived from algebraic splitting, were proposed in [3, 52]. We also mention [46] where an optimization problem is solved at each time-step to achieve continuity of stresses and continuity of velocity at the interface.

Recently, a novel loosely coupled partitioned scheme, called the "kinematically coupled β-scheme", was introduced in [11]. Because of its simple implementation, modularity, and good performance, the kinematically-coupled scheme and its modifications provide an appealing way to study multi-physics problems involving FSI. Indeed, this scheme has been used by several groups to study FSI problems in hemodynamics including poroelastic arterial walls [15], non-Newtonian fluids [40], cardiovascular stents [44], thin structures with longitudinal displacement [12, 45], FSI with thick structures [13], and FSI with multi-layered structure of arterial walls [43, 14]. See also [25, 29, 26] for a generalization of this scheme called "the incremental displacement-correction scheme." The kinematically-coupled β-scheme successfully deals with problems associated with the added mass effect in a way different from those reported above. It is a modification of the kinematically coupled scheme first introduced in [34]. The parameter β was introduced in [11] to increase the accuracy. This parameter distributes the fluid pressure between the fluid and structure sub-problems.

In [42] the authors used the kinematically-coupled scheme to prove the existence of a weak solution to a fully nonlinear FSI problem between an incompressible, viscous fluid and a thin structure modeled by either the elastic or viscoelastic shell equations. The existence proof is based on constructing approximate solutions using the kinematically-coupled scheme, and showing that the approximate solutions converge to a weak solution as the time-discretization tends to zero. This existence result relies on energy estimates, which show that in the kinematically-coupled scheme the energy of the coupled FSI problem is well-approximated by the discretized problem. A consequence of this result is that the kinematically-coupled scheme is stable.

In contrast with the energy estimates approach showing unconditional stability of the scheme, the present manuscript uses a different approach, similar to that of [18] (which was based on the Dirichlet-to-Neumann mapping applied to a simplified FSI problem), which reveals, explicitly, how and why this scheme is unconditionally stable for any $0 \leq \beta \leq 1$.

The theoretical results are confirmed by numerical simulations, applied to a fully nonlinear FSI benchmark problem in hemodynamics, originally presented in [31], and used for testing of various numerical schemes [5, 47, 3, 51, 34]. The hemodynamics and structure parameters in this benchmark problem fall into the critical regime for which the classical loosely-coupled Dirichlet-Neumann schemes are unstable. Our results show that the kinematically-coupled β-scheme is stable for those parameters, as predicted by the theory. We also show that the kinematically-couped β-scheme compares well with the simulations obtained using a monolithic scheme by Badia, Quaini, and Quarteroni [3, 51]. Further numerical results obtained using the kinematically-coupled β-scheme, and a comparison with experimental measurements can be found in [12].

This manuscript is organized as follows. We begin in Section 2 by a description of the kinematically-coupled β-scheme for a full FSI problem in which the structure is modeled by a cylindrical, linearly viscoelastic membrane shell model, also known as the 1D generalized string model. Then, the simplified FSI problem from [18] is introduced in Section 3, and a formulation of the kinematically coupled β-scheme applied to this simplified problem is presented. Stability analysis of the scheme applied to the simplified problem is presented in Section 4. Numerical results are presented in Section 5, where a fully nonlinear FSI benchmark problem, discussed in Section 2, is solved. Stability of the scheme is shown for the parameter values well within the range of instability of Dirichlet-Neumann schemes. A comparison with the stability analysis associated with classical Dirichlet-Neumann loosely coupled schemes is presented in Section 6.

2. Problem definition for a fully nonlinear FSI problem

We consider the flow of an incompressible, viscous fluid in a channel of radius R and length L, see Figure 1. To fix ideas we will be assuming that the channel is a subset of $\mathbb{R}^2$. Nothing in the splitting scheme, however, depends on the dimension of the problem, and the scheme can be applied to 3D problems as well, as was done in, e.g., [45]. The channel reference domain is denoted by $\Omega = (0, L) \times (-R, R)$ and the lateral boundary by

$$\Gamma = \{(z, r) \in \mathbb{R}^2 \mid 0 < z < L,\ r = \pm R\}.$$

The lateral boundary of the channel is assumed to be deformable, with negligible

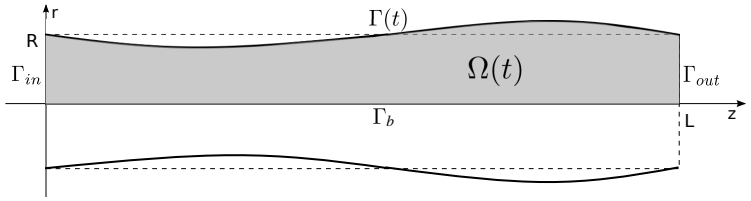

FIGURE 1. Deformed domain $\Omega(t)$.

longitudinal displacement. Without loss of generality, we consider only the upper half of the fluid domain with a symmetry boundary condition at the bottom boundary $r = 0$. The fluid domain, which depends on time, is not known *a priori*, and is denoted by

$$\Omega(t) = \{(z, r) \in \mathbb{R}^2 : z \in (0, L),\ r \in (0, R + \eta(z, t))\},$$

where η denotes the vertical (radial) displacement of the lateral boundary, namely,

$$\Gamma(t) = \{(z,r) \in \mathbb{R}^2 : r = R + \eta(z,t),\ z \in (0,L)\}.$$

The bottom portion of the boundary will be denoted by $\Gamma_b = (0,L) \times \{0\}$, with $\Gamma_{in} = \{0\} \times (0,R)$, $\Gamma_{out} = \{L\} \times (0,R)$ denoting the inlet and outlet parts, respectively.

We consider the flow of an incompressible, viscous fluid driven by the inlet and outlet pressure data $p_{in/out}(t)$, with the fluid velocity on $\Gamma(t)$ given by $w\mathbf{e}_r$, and the symmetry boundary condition at the bottom part of the boundary. Thus, the **fluid problem** reads: Find the fluid velocity $\boldsymbol{u} = (u_z(z,r,t), u_r(z,r,t))$ and pressure $p = p(z,r,t)$ such that

$$\left\{\begin{array}{rcll} \rho_f\big(\dfrac{\partial \mathbf{u}}{\partial t} + (\mathbf{u}\cdot\nabla)\mathbf{u}\big) &=& \nabla\cdot\boldsymbol{\sigma} & \text{in } \Omega(t),\ t \in (0,T), \\ \nabla\cdot\mathbf{u} &=& 0 & \text{in } \Omega(t), \\ u_r = 0,\ \dfrac{\partial u_z}{\partial r} &=& 0 & \text{on } \Gamma_b \times (0,T), \\ \boldsymbol{\sigma}\mathbf{n} &=& -p_{in/out}(t)\mathbf{n} & \text{on } \Gamma_{in/out} \times (0,T), \\ \mathbf{u} &=& w\mathbf{e}_r & \text{on } \Gamma(t),\ t \in (0,T), \end{array}\right. \tag{1}$$

where ρ_f is the fluid density, and $\boldsymbol{\sigma}$ is the fluid stress tensor; $\boldsymbol{\sigma} = -p\mathbf{I} + 2\mu\mathbf{D}(\mathbf{u})$ for a Newtonian fluid, where μ is the fluid viscosity and $\mathbf{D}(\mathbf{u}) = (\nabla\mathbf{u} + (\nabla\mathbf{u})^\tau)/2$ is the rate-of-strain tensor.

The **structure problem** is defined by solving an elastodynamics problem for a cylindrical linearly viscoelastic membrane shell, also known as a 1D generalized string model [54], capturing only vertical (radial) displacement $\eta = \eta(z,t)$ from the reference configuration:

$$\rho_s h\frac{\partial^2\eta}{\partial t^2} + C_0\eta - C_1\frac{\partial^2\eta}{\partial z^2} + D_0\frac{\partial\eta}{\partial t} - D_1\frac{\partial^3\eta}{\partial t\partial z^2} = f, \tag{2}$$

with the boundary conditions $\eta(0) = \eta(L) = 0$, and the initial condition given by the zero initial displacement and zero initial structure velocity. The coefficients ρ_s and h are the structure density and thickness, respectively, while the constants $C_i, D_i > 0, i = 1,2$, are the elastic and viscoelastic structural coefficients [17, 54].

The **coupling** between the fluid and structure is defined by the kinematic and dynamics lateral boundary conditions, respectively:

$$\begin{array}{rcl} (\dfrac{\partial\eta}{\partial t}(z,t), 0) &=& \boldsymbol{u}(z, R+\eta(z,),t), \\ f(z,t) &=& -J(z,t)(\boldsymbol{\sigma}\mathbf{n})(z, R+\eta(z,t),t)\cdot\mathbf{e}_r, \end{array} \tag{3}$$

where $J(z,t) = -\sqrt{1 + \left(\dfrac{\partial\eta}{\partial z}(z,t)\right)^2}$ denotes the Jacobian of the transformation from the Eulerian framework used to describe the fluid equations, to the Lagrangian coordinates used in the structure equations. Here f in (3) is defined by the left hand-side of (2). The kinematic lateral boundary condition describes continuity of velocities at the fluid-structure interface (the no-slip condition), while the dynamic lateral boundary condition describes the second Newton's Law of motion on $\Gamma(t)$.

2.1. The kinematically coupled β-scheme. To solve this problem numerically, we consider the kinematically coupled β-scheme, introduced in [11]. This scheme is based on the time-discretization via Lie operator splitting (see e.g., [33, 11]).

2.1.1. The Lie scheme. Let A be an operator from a Hilbert space H into itself, and suppose $\phi_0 \in H$. Consider the following initial-value problem:

$$\frac{\partial \phi}{\partial t} + A(\phi) = 0, \quad \text{in } (0,T), \quad \text{where} \quad A = \sum_{i=1}^{P} A_i, \quad \phi(0) = \phi_0. \tag{4}$$

The Lie scheme consists of splitting the full problem into P sub-problems, each defined by an operator $A_i, i = 1, ..., P$. The original problem is discretized in time with the time step $\Delta t > 0$, so that $t^n = n\Delta t$. The Lie splitting scheme consist of solving a series of problems $\frac{\partial \phi_i}{\partial t} + A_i(\phi_i) = 0$, for $i = 1, ..., P$, each defined over the entire time interval (t^n, t^{n+1}), but with the initial data for the i^{th} problem given by the solution of the $(i-1)^{st}$ problem at t^{n+1}. More precisely, set $\phi^0 = \phi_0$. Then, for $n \geq 0$ compute ϕ^{n+1} by solving

$$\frac{\partial \phi_i}{\partial t} + A_i(\phi_i) = 0 \quad \text{in } (t^n, t^{n+1}), \quad \phi_i(t^n) = \phi^{n+(i-1)/P}, \tag{5}$$

and then set $\phi^{n+i/P} = \phi_i(t^{n+1})$, for $i = 1, \ldots . P$. This method is first-order accurate in time. To increase the accuracy in time to second-order, a symmetrization of the scheme can be performed.

To perform the Lie splitting, problem (1)-(3) must first be written as a first-order system in time. To do this, we utilize the kinematic lateral boundary condition and express the time-derivative of η as the trace of the fluid velocity on Γ, $\mathbf{u}|_\Gamma \cdot \mathbf{e}_r$. The resulting system is then given by the following:

Problem 2.1. *Find* $(\mathbf{u}, p, \eta)$ *such that*

$$\begin{cases} \rho_f\big(\dfrac{\partial \mathbf{u}}{\partial t} + (\mathbf{u}\cdot\nabla)\mathbf{u}\big) = \nabla\cdot\boldsymbol{\sigma} & \text{in } \Omega(t),\ t\in(0,T), \\ \nabla\cdot\mathbf{u} = 0 & \text{in } \Omega(t), \\ u_r = 0, \quad \dfrac{\partial u_z}{\partial r} = 0 & \text{on } \Gamma_b \times (0,T), \\ \boldsymbol{\sigma}\mathbf{n} = -p_{in/out}(t)\mathbf{n} & \text{on } \Gamma_{in/out}\times(0,T), \\ \mathbf{u}|_{r=R+\eta} = \dfrac{\partial \eta}{\partial t}\mathbf{e}_r & \text{on } \Gamma,\ t\in(0,T), \\ \rho_s h \dfrac{\partial \mathbf{u}}{\partial t}\big|_\Gamma \cdot \mathbf{e}_r + C_0\eta - C_1\dfrac{\partial^2 \eta}{\partial z^2} & \\ +D_0\mathbf{u}|_\Gamma\cdot\mathbf{e}_r - D_1\dfrac{\partial^2(\boldsymbol{u}|_\Gamma)}{\partial z^2}\cdot\mathbf{e}_r = -J\boldsymbol{\sigma}\mathbf{n}|_\Gamma\cdot\mathbf{e}_r & \text{on } \Gamma\times(0,T). \end{cases}$$

To deal with the motion of the fluid domain, an Arbitrary Lagrangian-Eulerian (ALE) approach is used [37, 22, 47]. We introduce a family of (arbitrary, invertible, smooth) mappings A_t defined on the reference domain Ω such that for each $t \in [0,T]$, A_t maps the reference domain Ω onto the current domain $\Omega(t)$. Now, the ALE time-derivative of function f defined on $\Omega(t)\times(0,T)$ is given by

$$\left.\frac{\partial f}{\partial t}\right|_{\hat{\boldsymbol{x}}} = \frac{\partial f}{\partial t} + \mathbf{w}\cdot\nabla f, \tag{6}$$

where $\mathbf{w}$ denotes the domain velocity given by

$$\mathbf{w}(z,r,t) = \frac{\partial \mathcal{A}_t}{\partial t}(\hat{z},\hat{r}), \text{ where } (\hat{z},\hat{r}) = \mathcal{A}_t^{-1}(z,r). \tag{7}$$

Problem (1)-(3) can now be written in the following first-order ALE form (for more details please see [11]):

Problem 2.2. *Find* $(\mathbf{u}, p, \eta)$ *such that*

$$
\begin{cases}
\rho_f\big(\dfrac{\partial \mathbf{u}}{\partial t}\Big|_{\hat{\boldsymbol{x}}} + ((\mathbf{u}-\mathbf{w})\cdot\nabla)\mathbf{u}\big) &= \nabla\cdot\boldsymbol{\sigma} & \text{in } \Omega(t),\ t\in(0,T),\\
\nabla\cdot\mathbf{u} &= 0 & \text{in } \Omega(t),\\
u_r = 0,\quad \dfrac{\partial u_z}{\partial r} = 0 & & \text{on } \Gamma_b\times(0,T),\\
\boldsymbol{\sigma}\mathbf{n} &= -p_{in/out}(t)\mathbf{n} & \text{on } \Gamma_{in/out}\times(0,T),\\
\mathbf{u}|_{r=R+\eta} &= \dfrac{\partial \eta}{\partial t}\mathbf{e}_r & \text{on } \Gamma,\ t\in(0,T),\\
\rho_s h\dfrac{\partial(\mathbf{u}|_\Gamma)}{\partial t}\cdot\mathbf{e}_r + C_0\eta - C_1\dfrac{\partial^2\eta}{\partial z^2} & & \\
\quad + D_0\mathbf{u}|_\Gamma\cdot\mathbf{e}_r - D_1\dfrac{\partial^2(\mathbf{u}|_\Gamma)}{\partial z^2}\cdot\mathbf{e}_r &= -J\boldsymbol{\sigma}\mathbf{n}|_\Gamma\cdot\mathbf{e}_r & \text{on } \Gamma\times(0,T).
\end{cases}
$$

The strategy of the kinematically coupled scheme is to split this problem into a fluid sub-problem and a structure sub-problem in such a way that the inertia of the thin structure is coupled with the fluid sub-problem via a "Robin-type" boundary condition on $\Gamma(t)$. When the structure is viscoelastic, the structural viscosity can be treated together with the structure inertia as a part of the same boundary condition (i.e., all the terms in the structure equation involving the trace of fluid velocity on Γ can be used as a boundary condition for the fluid sub-problem). The elastodynamics of the structure problem is solved separately in the structure sub-problem.

Additionally, in the β-scheme a coefficient $\beta\in[0,1]$ is introduced (independent of time), and the fluid stress on Γ is split into two parts:

$$\boldsymbol{\sigma}\mathbf{n} = \underbrace{\boldsymbol{\sigma}\mathbf{n} + \beta p\mathbf{n}}_{(I)}\underbrace{-\beta p\mathbf{n}}_{(II)} \quad \text{on} \quad \Gamma,$$

where the case $\beta = 0$ corresponds to the classical kinematically coupled scheme introduced in [34]. Part I of the fluid stress is used in the fluid sub-problem, while Part II (the β-fraction of the pressure) is used to load the structure in the elastodynamics sub-problem. Thus, the dynamic coupling condition on Γ

$$
\begin{aligned}
\rho_s h\frac{\partial(\mathbf{u}|_\Gamma)}{\partial t}\cdot\mathbf{e}_r \;=\; & -C_0\eta + C_1\frac{\partial^2\eta}{\partial z^2} + \left(D_0\mathbf{u}|_\Gamma - D_1\frac{\partial^2(\mathbf{u}|_\Gamma)}{\partial z^2} - J\boldsymbol{\sigma}\mathbf{n}|_\Gamma - J\beta p\mathbf{n}|_\Gamma\right)\cdot\mathbf{e}_r\\
& + J\beta p\mathbf{n}|_\Gamma\cdot\mathbf{e}_r
\end{aligned}
$$

is split into the fluid part:

$$\rho_s h\frac{\partial(\mathbf{u}|_\Gamma)}{\partial t}\cdot\mathbf{e}_r = -D_0\mathbf{u}|_\Gamma\cdot\mathbf{e}_r + D_1\frac{\partial^2(\mathbf{u}|_\Gamma)}{\partial z^2}\cdot\mathbf{e}_r - J\boldsymbol{\sigma}\mathbf{n}|_\Gamma\cdot\mathbf{e}_r - J\beta p\mathbf{n}|_\Gamma\cdot\mathbf{e}_r, \tag{8}$$

and the structure part:

$$
\begin{aligned}
&\rho_s h\frac{\partial(\mathbf{u}|_\Gamma)}{\partial t}\cdot\mathbf{e}_r = -C_0\eta + C_1\frac{\partial^2\eta}{\partial z^2} + J\beta p\mathbf{n}|_\Gamma\cdot\mathbf{e}_r, \text{ with}\\
&\rho_s h\frac{\partial(\mathbf{u}|_\Gamma)}{\partial t}\cdot\mathbf{e}_r = \rho_s h\frac{\partial^2\eta}{\partial t^2}.
\end{aligned}
$$

This gives rise to the structure problem in terms of η, defined on Γ:

$$\rho_s h\frac{\partial^2\eta}{\partial t^2} + C_0\eta - C_1\frac{\partial^2\eta}{\partial z^2} = J\beta p\mathbf{n}|_\Gamma\cdot\mathbf{e}_r. \tag{9}$$

The splitting scheme is then defined by the following.

The geometry sub-problem:
Step 0. The fluid domain $\Omega(t^n)$ and ALE velocity $\mathbf{w}^{n+1/3}$ are calculated via, e.g.,:

$$\mathcal{A}_{t^n}(\hat{z},\hat{r}) = \left(\hat{z}, \frac{R}{R+\eta^n(\hat{z},t)}\hat{r}\right), \quad \Omega^f(t^n) = \mathcal{A}_{t^n}(\hat{\Omega}),$$

and

$$\mathbf{w}^{n+1/3} = \left(0, \frac{r^n - r^{n-1}}{\Delta t}\right),$$

where $(\hat{z},\hat{r}) \in \hat{\Omega}, r^n \in \Omega(t^n)$, and $r^{n-1} \in \Omega(t^{n-1})$.

The fluid sub-problem (Steps 1 and 2):
Step 1. A time-dependent Stokes problem is solved on the fixed fluid domain $\Omega(t^n)$ obtained in Step 0. The boundary condition at the lateral boundary is given by (8), with $\beta Jp\mathbf{n}$ taken explicitly from the previous time step. The displacement of the structure stays intact. The problem reads:
Given p^n, η^n, and $\mathbf{u}^n$ from the previous time step, find $\mathbf{u}^{n+1/3}$, p^{n+1}, $\eta^{n+1/3}$ such that:

$$\begin{cases} \rho_f \dfrac{\mathbf{u}^{n+1/3}-\mathbf{u}^n}{\Delta t} = \nabla\cdot\boldsymbol{\sigma}^{n+1/3}, \quad \nabla\cdot\mathbf{u}^{n+1/3} = 0 \quad \text{in } \Omega(t^n) \\ \rho_s h \dfrac{\mathbf{u}^{n+1/3}-\mathbf{u}^n}{\Delta t}|_\Gamma\cdot\mathbf{e}_r + D_0\mathbf{u}^{n+1/3}|_\Gamma\cdot\mathbf{e}_r - D_1\dfrac{\partial^2\mathbf{u}^{n+1/3}}{\partial z^2}|_\Gamma\cdot\mathbf{e}_r \\ +\sqrt{(1+\left(\frac{\partial\eta^n}{\partial z}\right)^2}(\boldsymbol{\sigma}^{n+1/3}\boldsymbol{n})\cdot\mathbf{e}_r = -\beta\sqrt{(1+\left(\frac{\partial\eta^n}{\partial z}\right)^2}p^n\mathbf{n}\cdot\mathbf{e}_r \quad \text{on } \Gamma, \\ \mathbf{u}^{n+1/3}\cdot\mathbf{e_z} = 0 \quad \text{on } \Gamma, \\ \eta^{n+1/3} = \eta^n \quad \text{in } \Gamma, \end{cases}$$

with the following boundary conditions:

$$\frac{\partial u_z^{n+1/3}}{\partial r}(z,0,t) = u_r^{n+1/3}(z,0,t) = 0 \quad \text{on } \Gamma_b,\ u_z^{n+1/3} = 0 \text{ on } \Gamma(t^n)$$

$$\mathbf{u}^{n+1/3}(0,R,t) = \mathbf{u}^{n+1/3}(L,R,t) = 0,$$

$$\boldsymbol{\sigma}^{n+1/3}\mathbf{n}|_{in} = -p_{in}(t^{n+1})\mathbf{n}|_{in} \text{ on } \Gamma_{\text{in}},\ \ \boldsymbol{\sigma}^{n+1/3}\mathbf{n}|_{out} = -p_{out}(t^{n+1})\mathbf{n}|_{out} \text{ on } \Gamma_{\text{out}}.$$

Step 2. Solve the fluid and ALE advection sub-problem defined on $\Omega(t^n)$, with the ALE velocity $\mathbf{w}^{n+1/3}$ defined by (2.1.1) based on the domain $\Omega(t^n)$ and the corresponding ALE mapping. The problem reads:
Find $\mathbf{u}^{n+2/3}$ and $\eta^{n+2/3}$ such that

$$\begin{cases} \dfrac{\mathbf{u}^{n+2/3}-\mathbf{u}^{n+1/3}}{\Delta t} + (\mathbf{u}^{n+1/3}-\mathbf{w}^{n+1/3})\cdot\nabla\mathbf{u}^{n+2/3} = 0, \quad \text{in } \Omega(t^n) \\ \eta^{n+2/3} = \eta^{n+1/3} \quad \text{on } \Gamma, \\ \mathbf{u}^{n+2/3}|_\Gamma = \mathbf{u}^{n+1/3}|_\Gamma \quad \text{on } \Gamma, \end{cases}$$

with the following boundary conditions:

$$\mathbf{u}^{n+2/3} = \mathbf{u}^{n+1/3} \ \text{ on } \Gamma_-^{n+1/3}(t^n), \text{ where}$$

$$\Gamma_-^{n+1/3}(t^n) = \{\mathbf{x}\in\mathbb{R}^2 | \mathbf{x}\in\partial\Omega(t^n), (\mathbf{u}^{n+1/3}-\mathbf{w}^{n+1/3})\cdot\mathbf{n} < 0\}.$$

The structure (elastodynamics) sub-problem (Step 3):
Step 3. Solve the elastodynamics problem (9) for the location of the deformable boundary by involving the elastic part of the structure which is loaded by Part II of the normal fluid stress. Additionally, the fluid and structure communicate via the kinematic lateral boundary condition which gives the velocity of the structure in terms of the trace of the fluid velocity, taken initially to be the value from the previous step. To discretize the elastodynamics problem in time, we use the θ–scheme (see [33] for details). The problem reads:
Given p^{n+1} computed in Step 1, and η^n obtained at the previous time step, find $\mathbf{u}^{n+1}$ *and* η^{n+1} *such that*

$$\begin{cases} \mathbf{u}^{n+1} = \mathbf{u}^n, \quad \textit{in } \Omega(t^n) \\ \\ \mathbf{u}^{n+1}|_{\Gamma(t^n)} \cdot \mathbf{e}_r = \dfrac{\eta^{n+1} - \eta^{n-1}}{2\Delta t} \quad \textit{on } \Gamma, \\ \\ \rho_s h \dfrac{\eta^{n+1} - 2\eta^n + \eta^{n-1}}{\Delta t^2} + C_0(\theta\eta^{n+1} + (1-2\theta)\eta^n + \theta\eta^{n-1}) \\ -C_1 \left(\theta \dfrac{\partial^2 \eta^{n+1}}{\partial z^2} + (1-2\theta)\dfrac{\partial^2 \eta^n}{\partial z^2} + \theta \dfrac{\partial^2 \eta^{n-1}}{\partial z^2} \right) = \beta \sqrt{(1 + \left(\dfrac{\partial \eta^n}{\partial z} \right)^2} \, p^{n+1} \mathbf{n} \cdot \mathbf{e}_r \quad \textit{on } \Gamma, \end{cases}$$

with the boundary conditions:

$$\eta^{n+1}|_{z=0,L} = 0.$$

Set $t^n = t^{n+1}$, and return to Step 0.

A block-diagram showing the main steps of the scheme is given in Figure 2.1.1. More details about the scheme can be found in [11].

3. The simplified test problem

We show that the kinematically coupled β-scheme is unconditionally stable when applied to the simplified problem considered in [18] as the simplest problem which captures the main features related to the instabilities in classical loosely-coupled schemes caused by the "added mass effect". The simplified problem consists of solving the time-dependent Stokes equations for an incompressible, inviscid fluid in a 2D channel with deformable walls, and with the elastodynamics equations given by the 1D generalized string model. Moreover, it is assumed that the displacement of the deformable wall is small enough so that it can be neglected in the fluid flow problem. In this case the geometry of the fluid domain is fixed while the small deformation of the boundary is calculated using the elastodynamics equations, which are coupled with the fluid flow through the kinematic and dynamic coupling conditions. Thus, the problem is defined on the reference fluid domain Ω with the lateral boundary Γ.

We will be assuming that the inlet and outlet pressure data, which are functions of time, are uniformly bounded. This is a reasonable assumption for the blood flow application, since the pressure is typically a periodic function of time, with a bounded amplitude.

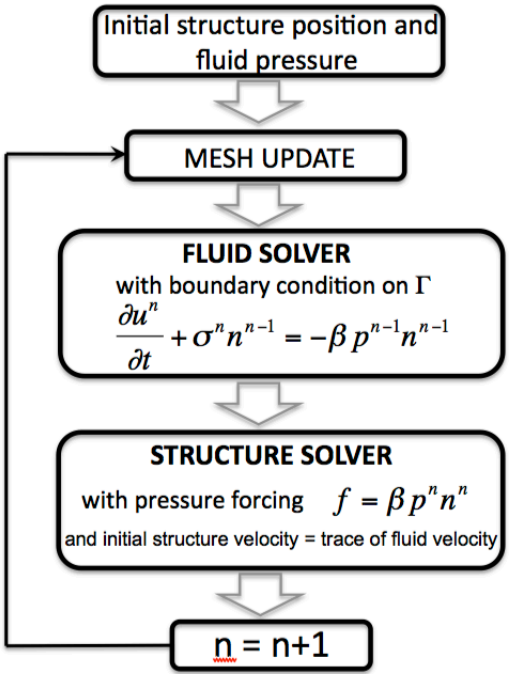

FIGURE 2. A block diagram showing the main steps of the kinematically coupled β-scheme.

The **fluid problem** reads: Find the fluid velocity $\boldsymbol{u} = \boldsymbol{u}(z, r, t)$ and pressure $p = p(z, r, t)$ such that

$$
\left\{
\begin{array}{rcll}
\rho_f \dfrac{\partial \boldsymbol{u}}{\partial t} + \nabla p &=& 0 & \text{in } \Omega \times (0,T), \\
\nabla \cdot \boldsymbol{u} &=& 0 & \text{in } \Omega \times (0,T), \\
\boldsymbol{u} \cdot \boldsymbol{n} &=& 0 & \text{on } \Gamma_b \times (0,T), \\
p &=& p_{in/out}(t) & \text{on } \Gamma_{in/out} \times (0,T), \\
\boldsymbol{u} \cdot \mathbf{e}_r &=& w & \text{on } \Gamma \times (0,T),
\end{array}
\right. \tag{10}
$$

with the initial velocity and pressure equal to zero.

The **structure problem** is defined by solving for $\eta = \eta(z, t)$ the 1D generalized string model:

$$
\rho_s h \frac{\partial^2 \eta}{\partial t^2} + C_0 \eta - C_1 \frac{\partial^2 \eta}{\partial z^2} = f, \tag{11}
$$

with boundary conditions $\eta(0) = \eta(L) = 0$, and initial conditions given by the zero initial displacement and zero initial structure velocity.

The **coupling** between the fluid and structure is defined by the kinematic and dynamic lateral boundary conditions, which, in this simplified problem, read:

$$
\begin{array}{rcl}
\left(\dfrac{\partial \eta}{\partial t}, 0\right) &=& \boldsymbol{u}|_\Gamma, \\
\rho_s h \dfrac{\partial^2 \eta}{\partial t^2} + C_0 \eta - C_1 \dfrac{\partial^2 \eta}{\partial z^2} &=& p|_\Gamma.
\end{array} \tag{12}
$$

The coupled fluid-structure interaction problem can be written as follows:

Problem 3.1.

$$
(13)\qquad \begin{cases} \rho_f \dfrac{\partial \boldsymbol{u}}{\partial t} + \nabla p = 0 & in\ \Omega \times (0,T), \\ \nabla \cdot \boldsymbol{u} = 0 & in\ \Omega \times (0,T), \\ \boldsymbol{u} \cdot \boldsymbol{n} = 0 & on\ \Gamma_b \times (0,T), \\ p = p_{in/out}(t) & on\ \Gamma_{in/out} \times (0,T), \\ \boldsymbol{u} \cdot \mathbf{e_r} = \dfrac{\partial \eta}{\partial t} & on\ \Gamma \times (0,T), \\ \rho_s h \dfrac{\partial^2 \eta}{\partial t^2} + C_0 \eta - C_1 \dfrac{\partial^2 \eta}{\partial z^2} = p & on\ \Gamma \times (0,T). \end{cases}
$$

To perform the Lie splitting, this system is written as a first-order system in time by using the kinematic coupling condition to replace $\rho_s h \dfrac{\partial^2 \eta}{\partial t^2}$ by $\rho_s h \dfrac{\partial \boldsymbol{u}}{\partial t}|_\Gamma \cdot \mathbf{e}_r$. As before, this point is crucial in order to perform the splitting which gives rise to a stable scheme. Namely, in the fluid sub-problem, which we write next, the structure inertia will be taken into account implicitly in the boundary condition on Γ, which is a crucial ingredient for the stability of the β-scheme. **This is a way how the fluid is coupled to the structure in this splitting.**

To simplify notation, as in [18], we introduce a linear, symmetric, positive definite operator $\mathcal{L}$ defined by the elasticity tensor associated with the structure problem. Namely, for $\eta, \xi \in H_0^1(0,L)$, we define

$$
(14)\qquad < \mathcal{L}\eta, \xi > := a_S(\eta, \xi),
$$

where $a_S(\eta, \xi)$ is the inner product on $H^1(0,L)$ defined by

$$
a_S(\eta, \xi) := \int_0^L C_0 \eta \xi dx + \int_0^L C_1 \frac{\partial \eta}{\partial x} \frac{\partial \xi}{\partial x} dx, \quad \forall \eta, \xi \in H^1(0,L).
$$

With this notation, the structure equation in Step 2 can be written as

$$
\rho_s h \frac{\partial^2 \eta}{\partial t^2} + \mathcal{L}\eta = p|_\Gamma.
$$

Notice that we are free to choose for the operator $\mathcal{L}$ any positive-definite operator associated with elastodynamics of thin structures, such as, for example, the full Koiter shell model operator, described in [17].

Before we write the main splitting steps we also notice that the fluid stress, which in this simplified example corresponds to the pressure, will be split into two parts: Part I which is given by $p - \beta p$, and Part 2 which is given by βp, so that $p = (p - \beta p) + \beta p$=Part 1 + Part 2.

Thus, the main steps of the Lie splitting for the simplified FSI problem (13) are:

The fluid sub-problem:

Step 1. The Stokes problem is solved on a fixed fluid domain, with a boundary condition which couples the structure inertia with Part I of the fluid stress. Here, the portion βp of the stress is taken explicitly, while the rest is taken implicitly. The displacement of the structure stays intact. The problem reads: *Given p^n from*

the previous time step, find $\mathbf{u}^{n+1/2}, \eta^{n+1/2}$ *and* p^{n+1} *such that:*

$$
\left\{
\begin{array}{rcll}
\rho_f \dfrac{\mathbf{u}^{n+1/2}-\mathbf{u}^n}{\Delta t} + \nabla p^{n+1} &=& 0 & \text{in } \Omega,\\
\nabla \cdot \mathbf{u}^{n+1/2} &=& 0 & \text{in } \Omega,\\
\mathbf{u}^{n+1/2}\cdot \boldsymbol{n} &=& 0 & \text{on } \Gamma_b,\\
p^{n+1} &=& p_{in/out}(t) & \text{on } \Gamma_{in/out},\\
\rho_s h \dfrac{\mathbf{u}^{n+1/2}-\mathbf{u}^n}{\Delta t}\big|_\Gamma - p^{n+1} &=& -\beta p^n. & \text{on } \Gamma,
\end{array}
\right. \tag{15}
$$

with the initial data for the fluid velocity on Γ*, namely,* $u^n|_\Gamma$*, given by the structure velocity calculated from the previous time-step. The structure displacement stays intact, namely*

$$
\eta^{n+1/2} = \eta^n \quad \text{on} \quad \Gamma. \tag{16}
$$

The structure sub-problem:

Step 2. The structure problem is solved with the pressure load βp^{n+1} just calculated from the fluid sub-problem. The problem reads: *Find* $\mathbf{u}^{n+1}$ *and* η^{n+1} *such that the following holds:*

$$
\left\{
\begin{array}{l}
\rho_s h \dfrac{\eta^{n+1}-2\eta^n+\eta^{n-1}}{\Delta t^2} + \mathcal{L}(\theta\eta^{n+1}+(1-2\theta)\eta^n+\theta\eta^{n-1}) = \beta p^{n+1}|_\Gamma \quad \text{on } \Gamma,\\
\mathbf{u}^{n+1}|_{\Gamma(t^n)}\cdot \mathbf{e}_r = \dfrac{\eta^{n+1}-\eta^{n-1}}{2\Delta t} \quad \text{on } \Gamma,
\end{array}
\right.
$$

with the initial data for the structure velocity given by the trace of the fluid velocity on Γ*, obtained from the just-calculated fluid sub-problem. The fluid velocity in* Ω *remains intact, namely:*

$$
\mathbf{u}^{n+1} = \mathbf{u}^{n+1/2} \quad \text{in } \Omega.
$$

The coupling of the two sub-problems through the initial data is the classical coupling provided by the Lie splitting scheme.

The pressure formulation:

In this simplified model, the problem is Step 1 can be entirely formulated in terms of the pressure and the normal trace of the fluid velocity on Γ. Namely, by taking the divergence free condition in the differentiated first (momentum) equation, the problem can be written in terms of the Laplace operator for the pressure. Similarly, we can re-write the boundary conditions on Γ in terms of the pressure and the normal trace of the velocity on Γ.

To simplify notation we will be using $\boldsymbol{n}$ to denote the normal on Γ (equal to $\mathbf{e}_r$), and $u_r|_\Gamma$ to denote the normal trace of the fluid velocity on Γ:

$$
\boldsymbol{n} := \mathbf{e}_r \text{ on } \Gamma \quad \text{and} \quad u_r|_\Gamma := \mathbf{u}|_\Gamma \cdot \mathbf{e}_r.
$$

With this, the problem is Step 1 can be stated as:

The fluid sub-problem in terms of p **and** $u_r|_\Gamma$

Step 1'. *Given* $u_r^n|_\Gamma$, p^n, η^n, *find* $p^{n+1/2}$, $u_r^{n+1/2}|_\Gamma$, $\eta^{n+1/2}$, *such that for* $t \in (t^n, t^{n+1})$:

$$
(17)\qquad \begin{cases} -\triangle p^{n+1/2} = 0, & \text{in } \Omega, \\ p^{n+1/2} = p_{in/out}(t) & \text{on } \Gamma_{in/out}, \\ \dfrac{\partial p^{n+1/2}}{\partial \boldsymbol{n}} = 0 & \text{on } \Gamma_b, \\ p^{n+1/2} + \dfrac{\rho_s h}{\rho_f}\dfrac{\partial p^{n+1/2}}{\partial \boldsymbol{n}} = \beta p^n & \text{on } \Gamma, \\ \text{-----------} & \\ \dfrac{u_r^{n+1/2}|_\Gamma - u_r^n|_\Gamma}{\Delta t} = -\dfrac{1}{\rho_f}\dfrac{\partial p^{n+1/2}|_\Gamma}{\partial \boldsymbol{n}} & \text{on } \Gamma, \\ \eta^{n+1/2} = \eta^n & \text{on } \Gamma, \end{cases}
$$

with the initial data for the fluid velocity on Γ given by the structure velocity calculated from the previous time-step.

The first four equations in Step 1 define a time-dependent Robin problem for the pressure (supplemented with the initial data for the pressure). The time-dependence enters through the inlet and outlet pressure data, which are functions of time. Notice that this problem already incorporates a portion of the coupling of the underlying FSI problem. This problem has a unique solution in the space $H^1(\Omega)$ provided that the data $p_{in/out} \in H^{1/2}(\Gamma_{in/out})$, and $p^n \in H^{-1/2}(\Gamma)$.

One can also show (see e.g., [18]) that the problem for the structure, defined in Step 2, has a unique solution $\eta \in H_0^1(0, L)$ provided that the initial data are such that $\eta|_{t=0} \in H_0^1(0, L)$, and $\partial\eta/\partial t|_{t=0} \in H_0^1(0, L)$, with $p^{n+1}|_\Gamma \in H^{1/2}(\Gamma)$.

Remark 3.1. *We emphasize that the fluid sub-problem in Step 1' is coupled to the structure sub-problem via the following two equations:*

- *The Robin boundary condition, given by the 4th equation in* (17). *This term accounts for the structure inertia, in an implicit way, via the kinematic coupling condition, and a portion of the dynamic coupling condition on* Γ. *This is exhibited, in particular, through the term* $\frac{\rho_s h}{\rho_f}\frac{\partial p^{n+1/2}}{\partial \boldsymbol{n}}$. *In this term,* $\rho_s h$ *is the structure mass, and* $\frac{\partial p^{n+1/2}}{\partial \boldsymbol{n}}$, *which was calculated from* $\frac{\partial p^{n+1/2}}{\partial \boldsymbol{n}} = -\rho_f \frac{\partial^2 \eta^{n+1/2}}{\partial t^2}$, *accounts for the structure inertia implicitly. If the structure inertia were taken into account explicitly, as is the case in Dirichlet-Neumann schemes, one would have the Neumann boundary condition* $\frac{\partial p^{n+1/2}}{\partial \boldsymbol{n}} = -\rho_f \frac{\partial^2 \eta^n}{\partial t^2}$ *for the pressure holding on* Γ, *given explicitly in terms of the structure velocity from the previous time-step, instead of the Robin condition. Our Robin boundary condition comes from: (1) using a portion of the dynamic coupling condition as dictated by the Lie splitting, through which the structure inertia* $\rho_s h \frac{\partial^2 \eta}{\partial t^2}$ *is included in the fluid sub-problem, and (2) using the kinematic coupling condition* $\frac{\partial^2 \eta}{\partial t^2} = \mathbf{u}|_\Gamma \cdot \mathbf{e}_r$ *to replace the structure velocity by the trace on the fluid velocity on* Γ *in an implicit way. By writing the problem in terms of the pressure, this boils down to using the condition* $\frac{\partial p^{n+1/2}}{\partial \boldsymbol{n}} = -\rho_f \frac{\partial^2 \eta^{n+1/2}}{\partial t^2}$ *in an implicit way, and not explicitly as in the Dirichlet-Neumann schemes. The implicit use of this condition leads to the fact that our fluid sub-problem, which includes structure inertia implicitly, can be written entirely in terms of the pressure. Thus, in this fluid sub-problem, the fluid and a portion of the structure equation are implicitly coupled via the implicit enforcement of the kinematic*

coupling condition, which leads to a fluid sub-problem for the pressure with a Robin-type boundary condition, which includes the structure inertia through the term multiplying $\rho_s h/\rho_f$.

- *The initial condition for the trace of the fluid velocity on Γ, which is given by the structure velocity calculated from the previous time-step.*

Likewise, the structure problem in Step 2 is coupled to the fluid problem given in Step 1' via:

- *the pressure loading term $\beta p^{n+1}|_\Gamma$, and*
- *through the initial data for the structure velocity, which is given by the trace of the fluid velocity from the just-calculated fluid sub-problem. The latter reflects the "standard" coupling provided by the Lie splitting scheme. Thus, even for $\beta = 0$, the structure "feels" the fluid via the initial condition for the structure velocity.*

4. Stability analysis

To study stability of the kinematically-coupled β-scheme we introduce the following operator: let $\mathcal{P} : H^{-1/2}(\Gamma) \to Q$, where

$$Q = \{q \in H^1(\Omega) \mid q|_{\Gamma_{in/out}} = 0\}, \tag{18}$$

such that

$$\begin{cases} -\triangle \mathcal{P}w &= 0, & \text{in } \Omega, \\ \mathcal{P}w &= 0 & \text{on } \Gamma_{in/out}, \\ \dfrac{\partial \mathcal{P}w}{\partial \boldsymbol{n}} &= 0 & \text{on } \Gamma_b, \\ \mathcal{P}w + \dfrac{\rho_s h}{\rho_f}\dfrac{\partial \mathcal{P}w}{\partial \boldsymbol{n}} &= w & \text{on } \Gamma. \end{cases} \tag{19}$$

Operator $\mathcal{P}$ associates to every $w \in H^{-1/2}(\Gamma)$ the solution of the pressure problem in Step 1', with the homogeneous inlet and outlet data $p_{in/out} = 0$.

We are interested in the trace on Γ of this pressure solution. For this purpose, introduce the operator $\mathcal{S} : H^{-1/2}(\Gamma) \to H^{1/2}(\Gamma)$ by

$$\mathcal{S}w = \mathcal{P}w|_\Gamma. \tag{20}$$

One can prove the following classical results (see e.g. [18, 53]):

Proposition 4.1. *Operator $\mathcal{S}$ satisfies the following properties:*

1. *$\mathcal{S} : H^{-1/2}(\Gamma) \to H^{1/2}(\Gamma)$ is continuous.*
2. *$\mathcal{S}$ is compact, self-adjoint, and positive on $L^2(\Gamma)$.*

Proof. Since this result is standard, we just outline the proof. We start by writing the weak formulation of problem (19) which reads: find $Pw \in Q$ such that

$$\int_\Omega \nabla Pw : \nabla \phi + \frac{\rho_f}{\rho_s h}\int_\Gamma Pw\phi = \frac{\rho_f}{\rho_s h}\langle w, \phi\rangle, \quad \forall \phi \in Q, \tag{21}$$

where $\langle w, \phi\rangle$ is a duality pairing between $H^{-1/2}(\Gamma)$ and $H^{1/2}(\Gamma)$. The first assertion (continuity) follows directly from here.

To show the second statement of the proposition, we consider $w, v \in L^2(\Gamma)$ and notice:

$$\int_\Gamma Swv = \int_\Gamma Pwv = \frac{\rho_s h}{\rho_f}\int_\Omega \nabla Pv : \nabla Pw + \int_\Gamma PvPw. \tag{22}$$

Here, the first equality follows from the definition of operator S. For the second equality we notice that $Pw \in Q$ is an admissible test function and, therefore, the

second equality is just formula (21) with the test function $\phi = Pw$. We now consider P as an operator on $L^2(\Gamma)$, i.e., $S : L^2(\Gamma) \to L^2(\Gamma)$. For every $w \in L^2(\Gamma)$, we have $Pw \in Q$. The trace theorem implies that $Sw = Pw|_\Gamma \in H^{1/2}(\Gamma)$, and so we have $\mathrm{Im}(S) \subseteq H^{1/2}(\Gamma)$. Since Γ is a bounded set, embedding $H^{1/2}(\Gamma) \hookrightarrow L^2(\Gamma)$ is compact, and thus S is a compact operator. Formula (22) implies that operator S is positive and self-adjoint, which completes the proof. $\square$

To study the solution of the corresponding non-homogeneous problem with $p = p_{in/out}(t)$ on $\Gamma_{in/out}$, we introduce an arbitrary continuous extension operator $E_F : H^{1/2}(\partial\Omega\backslash\Gamma) \to H^1(\Omega)$ so that $E_F q|_{\partial\Omega\backslash\Gamma} = q$ and $||E_F q||_{H^1(\Omega)} \le C||q||_{H^{1/2}(\partial\Omega\backslash\Gamma)}$. Let $p^* \in C(0,\infty; H^1(\Omega))$ be the solution to

$$\left\{\begin{array}{rcll} -\triangle p^* &=& \triangle E_F\bar{p}, & \text{in } \Omega, \\ p^* &=& 0 & \text{on } \Gamma_{in/out}, \\ \dfrac{\partial p^*}{\partial \boldsymbol{n}} &=& -\dfrac{\partial E_F\bar{p}}{\partial \boldsymbol{n}} & \text{on } \Gamma_b, \\ p^* + \dfrac{\rho_s h}{\rho_f}\dfrac{\partial p^*}{\partial \boldsymbol{n}} &=& -\dfrac{\partial E_F\bar{p}}{\partial \boldsymbol{n}} & \text{on } \Gamma, \end{array}\right.$$

where $\bar{p} = p_{in/out}$ on $\Gamma_{in/out}$. Now, the solution to the pressure problem in Step 1' is given by

$$p = p^* + E_F\bar{p} + \mathcal{P}(\beta p^n).$$

By denoting

$$p_{ext} = p^*|_\Gamma + E_F\bar{p}|_\Gamma$$

we can write the trace of the pressure solution in Step 1' on Γ as

$$p|_\Gamma = p_{ext} + \mathcal{S}(\beta p^n). \tag{23}$$

This trace of the pressure is used to load the equation for the structure in Step 2. Thus, the structure problem in Step 2 can now be written as: *Find η such that*

$$\rho_s h\frac{\partial^2\eta}{\partial t^2} + \mathcal{L}\eta = \beta(p_{ext}^{n+1} + \mathcal{S}(\beta p^n)). \tag{24}$$

We chose to discretize equation (24) in time using a θ-scheme discussed in [33]:

$$\rho_s h\frac{\eta^{n+1} - 2\eta^n + \eta^{n-1}}{\triangle t^2} + \mathcal{L}(\theta\eta^{n+1} + (1-2\theta)\eta^n + \theta\eta^{n-1}) = \beta(p_{ext}^{n+1} + \mathcal{S}(\beta p^n)). \tag{25}$$

It was shown in [33] that, for a given fixed right hand-side (source term), this scheme is stable for all $0 \le \theta \le 1/2$. Thus, we have unconditional stability with respect to the arbitrary ratios of the fluid and structure densities, provided that the right hand-side of this equation converges as $n \to \infty$.

A crucial point to observe here is that the right hand-side of this equation, which comes from the pressure loading, is given by an iterative procedure, and can be written entirely in terms of the initial pressure, the external pressure ($p_{in/out}$), and the operator $\mathcal{S}$ whose maximum eigenvalue, as we shall show below, is always less than 1, for all the choices of ρ_f and $\rho_s h$. Moreover, we will show below that the right hand-side converges, as the number of iterations $n \to \infty$, if $0 \le \beta \le 1$, for all the choices of ρ_f and $\rho_s h$.

To analyze the right hand-side of equation (24), we first study the eigenvalues of operator $\mathcal{S}$. As we shall see below, it is convenient to express the eigenvalues of $\mathcal{S}$ via the eigenvalues of the "Neumann to Dirichlet" operator $\mathcal{M}_A : H^{-1/2}(\Gamma) \to H^{1/2}(\Gamma)$ which is defined to be the trace on Γ of the operator $\mathcal{R} : H^{-1/2}(\Gamma) \to Q$:

$$\mathcal{M}_A w = \mathcal{R}w|_\Gamma, \tag{26}$$

where $\mathcal{R}$ associates to every $w \in H^{-1/2}(\Gamma)$ the solution $\mathcal{R}w \in Q$ of the following (pressure) problem:

$$\begin{cases} -\triangle \mathcal{R}w &= 0, & \text{in } \Omega, \\ \mathcal{R}w &= 0 & \text{on } \Gamma_{in/out}, \\ \dfrac{\partial \mathcal{R}w}{\partial \boldsymbol{n}} &= 0 & \text{on } \Gamma_b, \\ \dfrac{\partial \mathcal{R}w}{\partial \boldsymbol{n}} &= w & \text{on } \Gamma. \end{cases}$$

It can be shown (see [18]) that operator $\mathcal{M}_A : H^{-1/2}(\Gamma) \to H^{1/2}(\Gamma)$ is continuous, and that $\mathcal{M}_A$ is compact, self-adjoint, and positive on $L^2(\Gamma)$. Moreover, the eigenvalues μ_i of $\mathcal{M}_A$ are decreasing to zero ($\mu_i = L/(i\pi \tanh(i\pi R/L))$, i = 1,2,...), with the maximum eigenvalue μ_{max} given by

$$\mu_{max} = \mu_1 = \frac{L}{\pi \tanh\left(\dfrac{\pi R}{L}\right)}.$$

We will use this knowledge to calculate the eigenvalues of operator $\mathcal{S}$. Let μ be an eigenvalue of operator $\mathcal{M}_A$. Then, there exists a vector $v \neq 0$ such that

$$\mathcal{M}_A v = \mu v.$$

Recall that, by definition of $\mathcal{M}_A$, $\mathcal{M}_A v = \mathcal{R}v|_\Gamma$ and $\dfrac{\partial \mathcal{R}v}{\partial \boldsymbol{n}} = v$. Using this, we calculate

$$\mathcal{R}v|_\Gamma + \frac{\rho_s h}{\rho_f} \frac{\partial \mathcal{R}v}{\partial n}|_\Gamma = (\mu + \frac{\rho_s h}{\rho_f}) v|_\Gamma.$$

This implies that $\mathcal{R}v$ also satisfies the following Robin problem:

$$\begin{cases} -\triangle \mathcal{R}v &= 0, & \text{in } \Omega, \\ \mathcal{R}v &= 0 & \text{on } \Gamma_{in/out}, \\ \dfrac{\partial \mathcal{R}v}{\partial \boldsymbol{n}} &= 0 & \text{on } \Gamma_b, \\ \mathcal{R}v + \dfrac{\rho_s h}{\rho_f} \dfrac{\partial \mathcal{R}v}{\partial \boldsymbol{n}} &= \big(\mu + \dfrac{\rho_s h}{\rho_f}\big) v & \text{on } \Gamma. \end{cases}$$

We now notice that this is precisely the problem defined by the operator $\mathcal{P}$ in (19), with the data on Γ given by $(\mu + \frac{\rho_s h}{\rho_f})v$. Thus:

$$\mathcal{R}v = \mathcal{P}\big(\mu + \frac{\rho_s h}{\rho_f}\big) v,$$

and therefore, the traces on Γ satisfy:

$$\mathcal{M}_{\mathcal{A}} v = \mathcal{S}\big(\mu + \frac{\rho_s h}{\rho_f}\big) v = \big(\mu + \frac{\rho_s h}{\rho_f}\big) \mathcal{S}v.$$

Since $\mathcal{M}_A v = \mu v$ we finally get

$$\mu v = \big(\mu + \frac{\rho_s h}{\rho_f}\big) \mathcal{S}v.$$

Therefore, v is also an eigenvector for $\mathcal{S}$, and the corresponding eigenvalue λ satisfies:

$$\lambda = \frac{\mu}{\mu + \frac{\rho_s h}{\rho_f}}. \tag{27}$$

Thus, we have shown that the eigenvalues λ_i of $\mathcal{S}$ can be expressed using the eigenvalues μ_i of $\mathcal{M}_{\mathcal{A}}$ as

$$\lambda_i = \frac{\mu_i}{\mu_i + \dfrac{\rho_s h}{\rho_f}}, i = 1, 2, ... \tag{28}$$

We now use this information to study the right hand-side of equation (25). Since $\mathcal{S}$ is compact, there exists an orthonormal basis of $L^2(\Gamma)$ composed of the eigenvectors $\{z_j\}$ of $\mathcal{S}$. We thus expand the solution η, the external pressure data p_{ext}, and p^0, in this basis:

$$\eta^n = \sum_j (\eta^n)_j z_j, \quad p^n_{ext} = \sum_j (p^n_{ext})_j z_j, \quad p_0 = \sum_j (p_0)_j z_j.$$

Then, from (25), for each j, the Fourier coefficients satisfy the following equation:

$$\begin{aligned} \rho_s h \frac{(\eta^{n+1})_j - 2(\eta^n)_j + (\eta^{n-1})_j}{\triangle t^2} + \mathcal{L}(\theta(\eta_r^{n+1})_j + (1-2\theta)(\eta^n)_j + \theta(\eta^{n-1})_j) \\ = \beta((p^{n+1}_{ext})_j + \mathcal{S}(\beta(p^n))_j). \end{aligned} \tag{29}$$

The right hand-side of this equation is equal to

$$\begin{gathered} \beta((p^{n+1}_{ext})_j + \mathcal{S}(\beta(p^n))_j) = \\ \beta(p^{n+1}_{ext})_j + \textstyle\sum_{i=1}^n \beta^{i+1} \lambda_j^i (p^{n+1-i}_{ext})_j + \beta^{n+2} \lambda_j^{n+1} (p_0)_j. \end{gathered}$$

As $n \to \infty$, the series that defines the right hand-side converges if

$$|\beta \lambda_j| < 1.$$

From (28) we see that all λ_j are strictly less than one, which implies that the right hand-side converges if

$$0 \leq \beta \leq 1. \tag{30}$$

We have shown the following result:

Theorem 4.1. *The kinematically coupled β-scheme applied to a class of FSI problems represented by the simple benchmark problem* (13)*, is unconditionally stable for each β such that $0 \leq \beta \leq 1$.*

5. Numerical results

We present two numerical examples which show stability of the kinematically coupled β-scheme for a **fully nonlinear FSI problem**. The parameter values in the two examples are well within the range for which the classical Dirichlet-Neumann schemes are unstable. Numerical simulations in both cases are preformed on a benchmark problem by Formaggia et al. [31] used for testing of several FSI algorithms in hemodynamics applications [5, 47, 3, 51, 34].

Recall that results of [18] show that the classical loosely coupled, Dirichlet-Neumann scheme is unconditionally unstable if

$$\frac{\rho_s h}{\rho_f \mu_{max}} < 1, \tag{31}$$

where μ_{max} is the maximum eigenvalue of the added mass operator given by

$$\mu_{max} = \frac{L}{\pi \tanh\left(\frac{\pi R}{L}\right)}.$$

For the parameters given in Table 1, the value of μ_{max} is 7.46, so the critical value for the structure density is $\rho_s = 74.6$ g/cm^3. Therefore, the classical Dirichlet-Neumann scheme is unconditionally unstable if $\rho_s < 74.6$ g/cm^3. In Example 1, we

take the density of the structure to be 70-times smaller, given by the physiologically relevant value of $\rho_s = 1.1$ g/cm^3. We compare our results with the results obtained using a monolithic scheme by Badia, Quaini and Quarteroni [3, 51] showing excellent agreement. In Example 2, we choose an even smaller structural density, $\rho_s = 0.55$ g/cm^3, which is roughly half the value of the fluid density, therefore, capturing the case when $\rho_s < \rho_f$. Our results show that the scheme is stable even when the structure is lighter than the fluid.

The benchmark problem [31]**:**
The benchmark problem consists of solving the fully nonlinear FSI problem (1)-(3) with the values of the coefficients for the fluid problem given in Table 1, and the values of the structural coefficients given in Table 2.

Parameters	**Values**	**Parameters**	**Values**
Radius R (cm)	0.5	**Length** L (cm)	6
Fluid density ρ_f (g/cm^3)	1	**Dyn. viscosity** μ (poise)	0.035
Young's mod. E(dynes/cm^2)	0.75×10^6	**Wall thickness** h (cm)	0.1
Poisson's ratio σ	0.5		

TABLE 1. Parameter values used in Examples 1 and 2 presented in this section.

Coefficients	**Values**	**Coefficients**	**Values**
C_0	4×10^5	C_1	2.5×10^4
D_0	0	D_1	0.01

TABLE 2. The values of the coefficients in (2) used in Examples 1 and 2 below.

The flow is driven by the time-dependent pressure data:

$$p_{in}(t) = \begin{cases} \frac{p_{max}}{2}\left[1 - \cos\left(\frac{2\pi t}{t_{max}}\right)\right] & \text{if } t \le t_{max} \\ 0 & \text{if } t > t_{max} \end{cases}, \quad p_{out}(t) = 0 \ \forall t \in (0, T), \tag{32}$$

where $p_{max} = 2 \times 10^4$ (dynes/cm^2) and $t_{max} = 0.005$ (s). The graph of the inlet pressure data versus time is shown in Figure 3. The inlet and outlet boundary

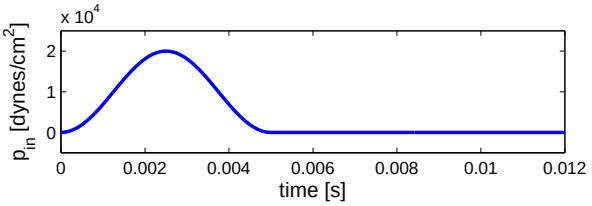

FIGURE 3. The inlet pressure pulse for Examples 1 and 2. The outlet pressure is kept at 0.

conditions for the structure are the absorbing boundary conditions:

$$\frac{\partial \eta_r}{\partial t} - \sqrt{\frac{C_1}{\rho_s}}\frac{\partial \eta_r}{\partial z} = 0 \quad \text{at } z = 0 \tag{33}$$

$$\frac{\partial \eta_r}{\partial t} + \sqrt{\frac{C_1}{\rho_s}}\frac{\partial \eta_r}{\partial z} = 0 \quad \text{at } z = L. \tag{34}$$

To deal with the motion of the fluid domain, we used the ALE mapping defined by the harmonic extension of the mapping that maps the boundary of Ω onto the boundary of $\Omega(t)$, for a given time t.

Parameter β, introduced in (30), which appears in Step 1 and Step 3 of our numerical scheme, and is independent of time, was taken to be $\beta = 1$. It was numerically observed in [11] that the change in β is associated with the change in accuracy of the scheme (not the stability), where the value of $\beta = 1$ provides the highest accuracy for this benchmark problem. We believe that the main reason for the gain in accuracy at $\beta = 1$ is the strong coupling between the fluid pressure (which incorporates the leading effect of the fluid loading onto the structure) and the structure elastodynamics, which is established for $\beta = 1$ in Step 3 of the splitting, described above.

5.1. Example 1: $\rho_s = 1.1$ g/cm^3. We solved the fully nonlinear benchmark problem described above over the time interval $[0, 0.012]$s. This time interval was chosen to be the same as in [31]. The end-point of this time interval corresponds to the time it takes a forward-moving pressure wave to reach the end of the fluid domain. The numerical results obtained using the kinematically coupled β-scheme were compared with the numerical results obtained using the monolithic scheme by Badia, Quaini and Quarteroni [3, 51]. Figures 4, 5 and 6 show a comparison

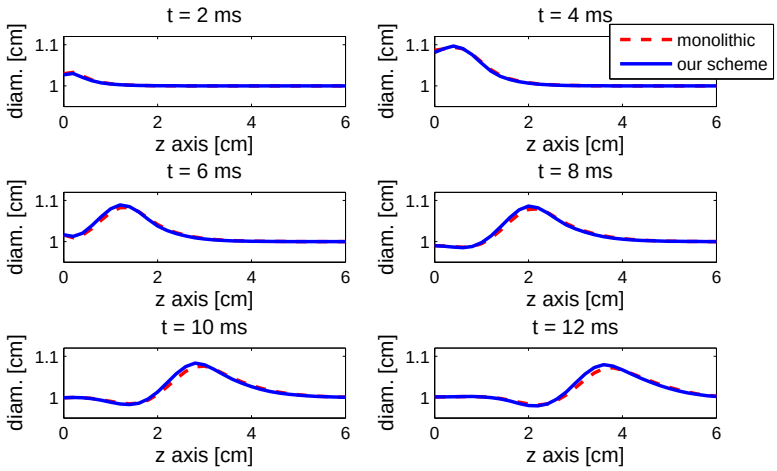

FIGURE 4. Example 1: Diameter of the tube computed with the kinematically coupled β-scheme (solid line) and with the monolithic scheme used by Quaini in [3, 51] (dashed line). The time step $\triangle t = 10^{-4}$ is used in both cases.

between tube diameter, flowrate and mean pressure, respectively, at six different

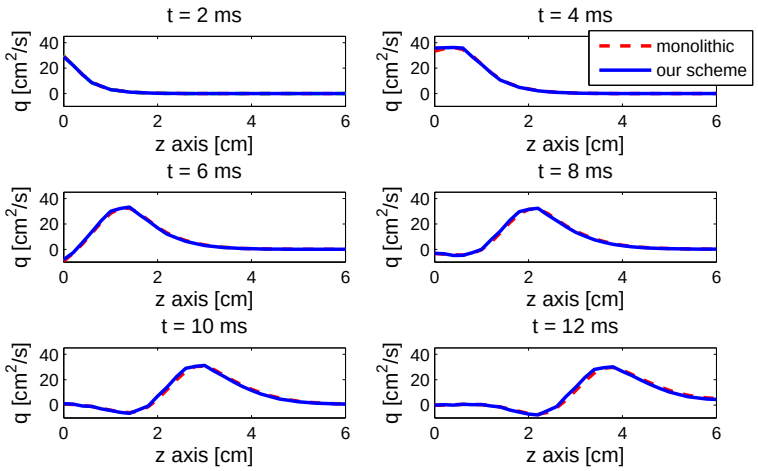

FIGURE 5. Example 1: Flowrate computed with the kinematically coupled β-scheme (solid line) and with the monolithic scheme used by Quaini in [3, 51] (dashed line). The time step $\triangle t = 10^{-4}$ in both cases.

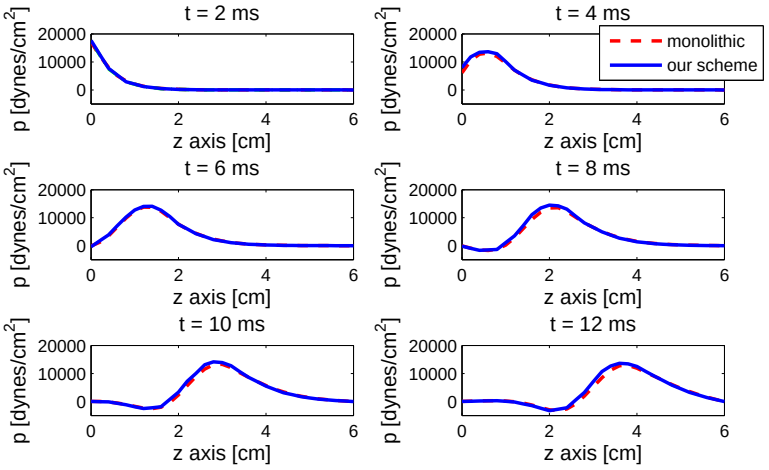

FIGURE 6. Example 1: Mean pressure computed with the kinematically coupled β-scheme (solid line) and with the monolithic scheme used by Quaini in [3, 51] (dashed line). The time step $\triangle t = 10^{-4}$ is used in both cases.

times. These results were obtained on the same mesh as the one used for the monolithic scheme in [51], containing 31×11 $\mathbb{P}_1$ fluid nodes. More preciesely, we used an isoparametric version of the Bercovier-Pironneau element spaces, also known as the $\mathbb{P}_1$-iso-$\mathbb{P}_2$ approximation, in which a coarse mesh is used for the pressure (mesh size h_p) and a fine mesh for the velocity (mesh step $h_v = h_p/2$).

The time step used was $\triangle t = 10^{-4}$, which is the same as the time step used for the monolithic scheme. Due to the splitting error, it is well-known that classical splitting schemes usually require smaller time step to achieve the accuracy comparable to that of monolithic schemes. However, the new splitting with $\beta = 1$ allows us to use the same time step as in the monolithic method, obtaining comparable accuracy, as shown in [11] and in Figure 7.

The reference solution was defined to be the one obtained with $\triangle t = 10^{-6}$. We calculated the relative and absolute L^2 errors for the velocity, pressure and displacement between the reference solution and the solutions obtained using $\triangle t = 5 \times 10^{-6}, 10^{-5},\ 5 \times 10^{-5}$ and 10^{-4}. Table 3 shows the relative error and the convergence rates for the pressure, velocity, and displacement obtained by the kinematically-coupled β-scheme. The graphs in Figure 7 show the absolute error and the convergence in time of the kinematically-coupled β-scheme and the monolithic scheme by Badia, Quaini and Quarteroni [3, 51].

$\triangle t$	$\frac{\|\|p-p_{ref}\|\|_{L^2}}{\|\|p_{ref}\|\|_{L^2}}$	L^2 order	$\frac{\|\|\boldsymbol{u}-\boldsymbol{u}_{ref}\|\|_{L^2}}{\|\|\boldsymbol{u}_{ref}\|\|_{L^2}}$	L^2 order	$\frac{\|\|\boldsymbol{\eta}-\boldsymbol{\eta}_{ref}\|\|_{L^2}}{\|\|\boldsymbol{\eta}_{ref}\|\|_{L^2}}$	L^2 order
10^{-4}	0.0251	-	0.0223	-	0.0392	-
5×10^{-5}	0.013	1.35	0.0151	0.56	0.0175	1.1
10^{-5}	0.0024	1.04	0.0038	0.87	0.0038	0.92
5×10^{-6}	0.0011	1.14	0.0017	1.12	0.0017	1.13

TABLE 3. Example 1: Convergence in time calculated at $t = 10$ ms.

5.2. Example 2: $\rho_s = 0.55$ g/cm^3. We consider the same test case as in Example 1, but now with the value for the structure density $\rho_s = 0.55$ g/cm^3. The problem is solved on the time interval $[0, 0.012]$s and with the same mesh as the one used in Example 1. Figures 8, 9 and 10 show the values of the tube diameter, flowrate and mean pressure, respectively, at six different times, obtained with $\triangle t = 10^{-4}$.

Finally, to show the convergence of the scheme, we define the reference solution to be the one obtained with $\triangle t = 10^{-6}$. We calculated the relative L^2 errors for the velocity, pressure and displacement between the reference solution and the solutions obtained using $\triangle t = 5 \times 10^{-6}, 10^{-5},\ 5 \times 10^{-5}$ and 10^{-4}. Table 4 shows the convergence rates for the pressure, velocity, and displacement obtained by the kinematically-coupled β-scheme. Thus, we see that the scheme performs well for a range of parameters for which the classical loosely-coupled, Dirichlet-Neumann scheme is unconditionally unstable.

$\triangle t$	$\frac{\|\|p-p_{ref}\|\|_{L^2}}{\|\|p_{ref}\|\|_{L^2}}$	L^2 order	$\frac{\|\|\boldsymbol{u}-\boldsymbol{u}_{ref}\|\|_{L^2}}{\|\|\boldsymbol{u}_{ref}\|\|_{L^2}}$	L^2 order	$\frac{\|\|\boldsymbol{\eta}-\boldsymbol{\eta}_{ref}\|\|_{L^2}}{\|\|\boldsymbol{\eta}_{ref}\|\|_{L^2}}$	L^2 order
10^{-4}	0.0239	-	0.0427	-	0.0749	-
5×10^{-5}	0.0096	1.32	0.0286	0.58	0.0408	0.87
10^{-5}	0.0017	1.06	0.0067	0.9	0.0079	1.021
5×10^{-6}	7.72e − 04	1.15	0.0031	1.13	0.0035	1.16

TABLE 4. Example 2: Convergence in time calculated at $t = 10$ ms.

6. Comparison with the Dirichlet-Neumann Scheme

We conclude this manuscript by comparing the kinematically-coupled β-scheme, summarized in (24), with the classical Dirichlet-Neumann scheme exhibiting the

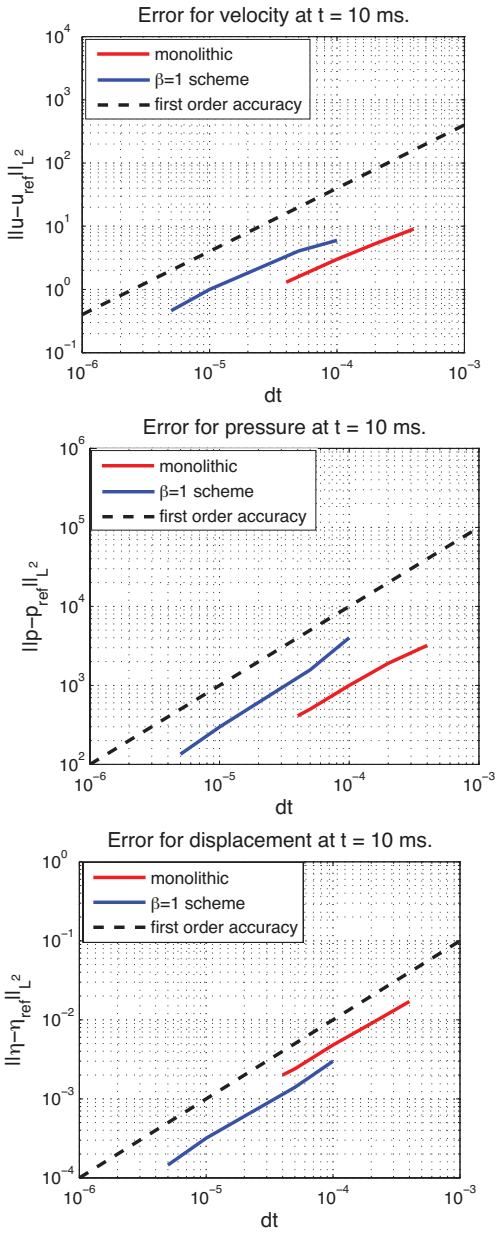

FIGURE 7. Example 1: The figures show absolute errors compared with the monolithic scheme. Top left: Error for fluid velocity at t=10 ms. Top right: Error for fluid pressure at t=10 ms. Bottom: Error for displacement at t=10 ms, [11]. Both schemes are first-order accurate in time, with comparable accuracy (notice the higher accuracy of the kinematically-coupled β scheme for the displacement).

"added mass effect." Equation (24) can be solved in an implicit way (written with

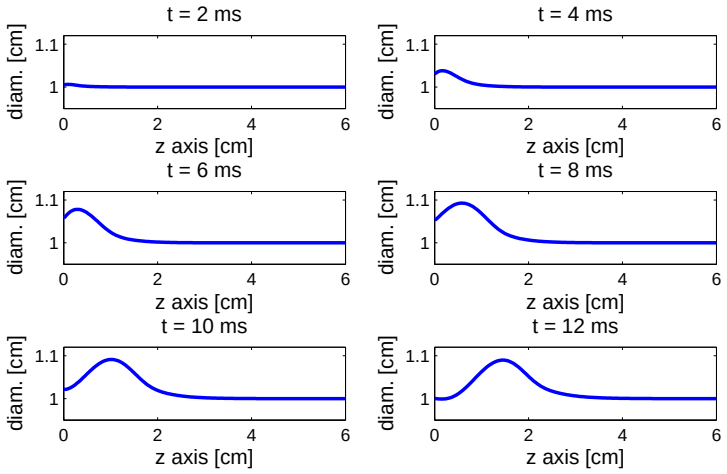

FIGURE 8. Example 2: Diameter of the tube computed with the kinematically coupled β-scheme, obtained with the time step $\triangle t = 10^{-4}$.

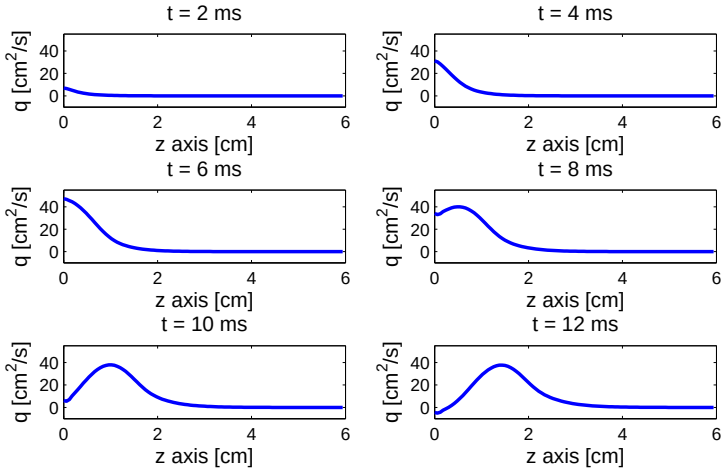

FIGURE 9. Example 2: Flowrate computed with the kinematically coupled β-scheme, obtained with the time step $\triangle t = 10^{-4}$.

a slight abuse of notation) as:

$$\rho_s h \frac{\partial^2 \eta^{n+1}}{\partial t^2} + \mathcal{L}\eta^{n+1} = \beta(p_{ext}^{n+1} + \mathcal{S}(\beta p^n)). \tag{35}$$

The corresponding equation resulting from the classical Dirichlet-Neumann scheme can be written as follows. We recall that the Dirichlet-Neumann scheme solves the FSI problem (10)-(12) by solving the fluid sub-problem (10) with Dirichlet boundary data for the fluid velocity on Γ, given in terms of the structure velocity $\partial\eta/\partial t$, calculated from the previous time step, and then uses the fluid stress, calculated

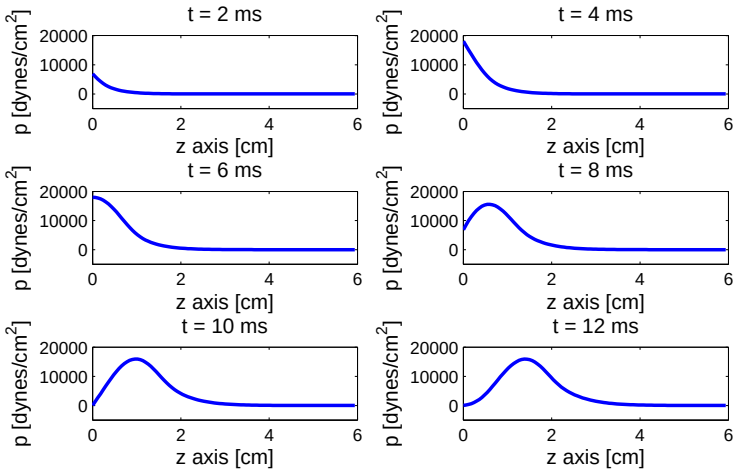

FIGURE 10. Example 2: Mean pressure computed with the kinematically coupled β-scheme, obtained with the time step $\triangle t = 10^{-4}$.

in problem (10), to load the structure in sub-problem (11). Figure 11 left shows a block diagram summarizing the main steps.

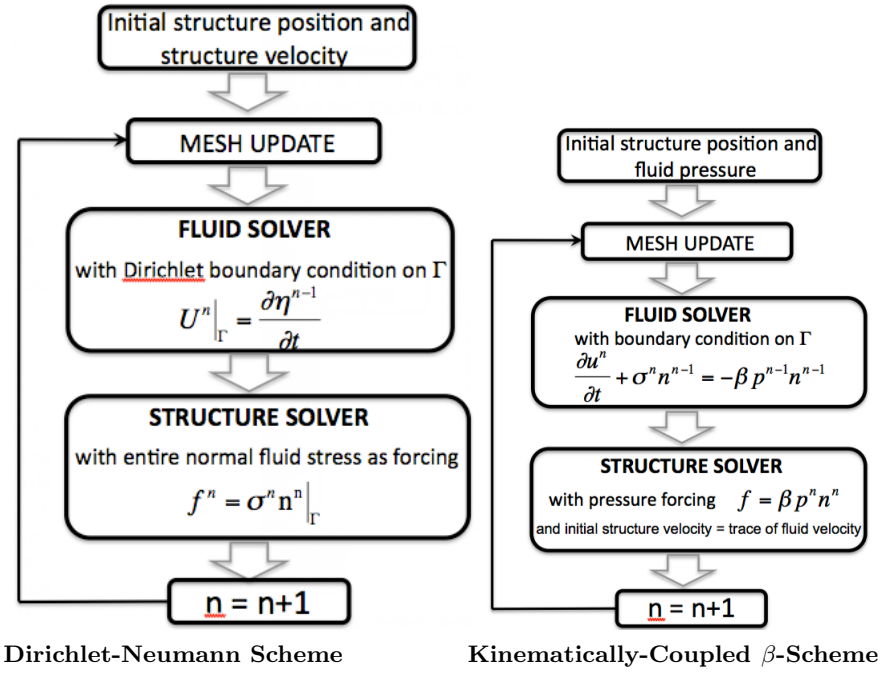

FIGURE 11. Left: Block diagram showing the main steps of a Dirichlet-Neumann scheme. Right: Block diagram showing the main steps of the kinematically-coupled β-scheme.

Using similar ideas as already presented in this manuscript, it was shown in [18] that this kind of partitioned approach leads to solving the problem for η of the form

$$\rho_s h \frac{\partial^2 \eta}{\partial t^2} + \mathcal{L}\eta = p|_\Gamma, \tag{36}$$

where

$$p|_\Gamma = p_{ext} - \rho_f \mathcal{M}_A \frac{\partial^2 \eta}{\partial t^2}. \tag{37}$$

Here p_{ext} comes from the "external" pressure data ($p_{in/out}$), and $\mathcal{M}_A$ is the "added mass operator" introduced in the previous section by formula (26).

While in the Dirichlet-Neumann loosely coupled scheme the w in the definition of operator R (formula (27)) corresponds to structure inertia $\partial^2\eta/\partial t^2$, in our kinematically coupled β-scheme w corresponds to the fraction of the fluid stress determined by βp. When $\beta = 0$, which corresponds to the original kinematically coupled scheme, this term is zero. We emphasize again that the structure inertia in the kinematically coupled schemes is taken *implicitly* in the Robin boundary condition, and not explicitely, as in the Dirichlet-Neumann schemes.

Using the added mass operator, the problem for the structure (36) can now be written as

$$(\rho_s h + \rho_f \mathcal{M}_A) \frac{\partial^2 \eta}{\partial t^2} + \mathcal{L}\eta = p_{ext}. \tag{38}$$

Since in the Dirichlet-Neumann loosely coupled partitioned schemes the pressure is calculated in the fluid sub-problem using the structure velocity from the previous time step, this implies that, with a slight abuse of notation, (38) can be written as

$$\rho_s h \frac{\partial^2 \eta^{n+1}}{\partial t^2} + \rho_f \mathcal{M}_A \frac{\partial^2 \eta^n}{\partial t^2} + \mathcal{L}\eta^n = p_{ext}. \tag{39}$$

More precisely, equation (39) means

$$\rho_s h \frac{\eta^{n+1} - 2\eta^n + \eta^{n-1}}{(\Delta t)^2} + \rho_f \mathcal{M}_A \frac{\eta^n - 2\eta^{n-1} + \eta^{n-2}}{(\Delta t)^2} + \mathcal{L}\eta^n = p_{ext}. \tag{40}$$

It was shown in [18] that this scheme is unconditionally unstable if

$$\frac{\rho_s h}{\rho_f \mu_{max}} < 1, \tag{41}$$

where μ_{max} is the maximum eigenvalue of the added mass operator $\mathcal{M}_A$. It was also shown in [18] that the maximum eigenvalue μ_{max} is associated with the aspect ratio of the fluid domain R/L. The smaller that aspect ratio (the more slender the domain), the larger the maximum eigenvalue μ_{max}.

Going back to equation (35), one can now see that there is no added mass operator associated with the kinematically coupled β-scheme. The right hand side of equation (35) is an iterative procedure which can be written in terms of the initial pressure and of the external (in/out) pressure data, which, we showed, converges for $0 \leq \beta \leq 1$. Thus, for $0 \leq \beta \leq 1$, the kinematically coupled β-scheme does not suffer from the added mass effect for any choice of the parameters in the problem. A side-by-side comparison between the two schemes is shown in the block-diagrams in Figure 11.

7. Conclusions

This manuscript shows the main reasons for the unconditional stability of the kinematically-coupled β-scheme, used in [11, 12, 13, 15, 34, 40, 42, 43, 44, 45] to studycf several different FSI problems in hemodynamics. The inclusion of the structure inertia into the fluid sub-problem implicitly, giving rise to a Robin-type boundary condition for the fluid sub-problem, is the main reason for the unconditional stability of the scheme. This is in contrast with the classical Dirichlet-Neumann loosely-coupled schemes, for which the structure inertia is included in the fluid sub-problem explicitly, via a Dirichlet boundary condition describing the no-slip condition at the fluid-structure interface. Modularity, simple implementation, and unconditional stability without the need for sub-iterations at each time-step, make this scheme particularly appealing for numerical simulation of multi-physics problems arising in biological fluid-structure interaction.

References

[1] M. Astorino, F. Chouly, and M.A. Fernández. An added-mass free semi-implicit coupling scheme for fluid-structure interaction. *Comptes Rendus Mathematique*, 347(1-2):99–104, 2009.

[2] M. Astorino, F. Chouly, and M.A. Fernández Varela. Robin based semi-implicit coupling in fluid-structure interaction: Stability analysis and numerics. *SIAM J. Sci. Comput.*, 31:4041–4065, 2009.

[3] S. Badia, A. Quaini, and A. Quarteroni. Splitting methods based on algebraic factorization for fluid-structure interaction. *SIAM J. Sci. Comput.* 30(4):7027–7051, 2008.

[4] S. Badia, A. Quaini, and A. Quarteroni. Coupling Biot and Navier-Stokes equations for modelling fluid-poroelastic media interaction. *J. Comput. Phys.* 228(21):7986–8014, 2009.

[5] S. Badia, F. Nobile, C. Vergara. Fluid-structure partitioned procedures based on Robin transmission conditions. *J. Comput. Phys.* 227:7027–7051, 2008.

[6] S. Badia, F. Nobile, and C. Vergara. Robin-Robin preconditioned Krylov methods for fluid-structure interaction problems. *Comput. Methods Appl. Mech. Eng.*, 198(33-36):2768–2784, 2009.

[7] V. Barbu, Z. Grujić, I. Lasiecka, and A. Tuffaha. Smoothness of weak solutions to a nonlinear fluid-structure interaction model. *Indiana Univ. Math. J.*, 57(3):1173–1207, 2008.

[8] Y. Bazilevs, V.M. Calo, T.J.R. Hughes, Y. Zhang. Isogeometric fluid-structure interaction: theory algorithms and computations. *Comput. Mech.* 43:3-37, 2008.

[9] Y. Bazilevs, V.M. Calo, Y. Zhang, T.J.R. Hughes. Isogeometric fluid-structure interaction analysis with applications to arterial blood flow *Comput. Mech.* 38 (4-5): 310–322, 2006.

[10] H. B. da Veiga. On the existence of strong solutions to a coupled fluid-structure evolution problem. *J. Math. Fluid Mech.*, 6(1):21–52, 2004.

[11] M. Bukač, S. Čanić, R. Glowinski, J. Tambača, and A. Quaini. Fluid-structure interaction in blood flow capturing non-zero longitudinal structure displacement. *Journal of Computational Physics*, 2012; **235**:515-541

[12] Bukač, M. and Čanić, S. Longitudinal displacement in viscoelastic arteries: a novel fluid-structure interaction computational model, and experimental validation. *Journal of Mathematical Biosciences and Engineering* 10(2):258–388, 2013.

[13] M. Bukač, S. Čanić, R. Glowinski, B. Muha, and A. Quaini. A modular, operator splitting scheme for fluid-structure interaction problems with thick structures. *International Journal for Numerical Methods in Fluids*, In press 2013. DOI:10.1002/fld.3863

[14] M. Bukač, S. Čanić, B. Muha. A partitioned scheme for fluid-composite structure interaction problems. *Submitted*, 2013.

[15] M. Bukač, P. Zunino, and I. Yotov. Explicit partitioning strategies for interaction of the fluid with a multilayered poroelastic structure: An operator-splitting approach. *Submitted*, 2013.

[16] E. Burman and M. A. Fernández. Stabilization of explicit coupling in fluid-structure interaction involving fluid incompressibility. *Comput. Methods Appl. Mech. Eng.*, 198:766–784, 2009.

[17] S. Čanić, J. Tambača, G. Guidoboni, A. Mikelić, C. J. Hartley, and D. Rosenstrauch. Modeling viscoelastic behavior of arterial walls and their interaction with pulsatile blood flow. *SIAM J. Appl. Math.*, 67(1):164–193 (electronic), 2006.

[18] P. Causin, J. Gerbeau, and F. Nobile. Added-mass effect in the design of partitioned algorithms for fluid-structure problems. *Comput. Methods Appl. Mech. Eng.*, 194(42-44):4506–4527, 2005.

[19] M. Cervera, R. Codina, M. Galindo. On the computational efficiency and implementation of block-iterative algorithms for nonlinear coupled problems. *Eng. Comput.* 13 (6): 4–30, 1996.

[20] C. H. A. Cheng and S. Shkoller. The interaction of the 3D Navier-Stokes equations with a moving nonlinear Koiter elastic shell. *SIAM J. Math. Anal.*, 42(3):1094–1155, 2010.

[21] D. Coutand and S. Shkoller. The interaction between quasilinear elastodynamics and the Navier-Stokes equations. *Arch. Ration. Mech. Anal.*, 179(3):303–352, 2006.

[22] J. Donea. Arbitrary Lagrangian-Eulerian finite element methods, in: Computational methods for transient analysis. North-Holland, Amsterdam, 1983.

[23] S. Deparis, M. Fernández, L. Formaggia. Acceleration of a fixed point algorithm for a fluid-structure interaction using transpiration condition. em Math. Model. Numer. Anal. 37 (4): 601–616, 2003.

[24] B. Desjardins, M. J. Esteban, C. Grandmont, and P. Le Tallec. Weak solutions for a fluid-elastic structure interaction model. *Rev. Mat. Complut.*, 14(2):523–538, 2001.

[25] M. A. Fernández. Incremental displacement-correction schemes for the explicit coupling of a thin structure with an incompressible fluid. *C. R. Math. Acad. Sci. Paris*, 349(7-8):473–477, 2011.

[26] M. A. Fernández. Incremental displacement-correction schemes for incompressible fluid-structure interaction: stability and convergence analysis. *Numerische Mathematik*, 2012.

[27] M.A. Fernández, J.F. Gerbeau, and C. Grandmont. A projection algorithm for fluid-structure interaction problems with strong added-mass effect. *Comptes Rendus Mathematique*, 342(4):279–284, 2006.

[28] M. Fernández, J.-F. Gerbeau, C. Grandmont. A projection semi-implicit scheme for the coupling of an elastic structure with an incompressible fluid. *Int. J. Numer. Methods Eng.* 69 (4) : 794–821, 2007.

[29] M. A. Fernández and J. Mullaert. Displacement-velocity correction schemes for incompressible fluid-structure interaction. *C. R. Math. Acad. Sci. Paris*, 349(17-18):1011–1015, 2011.

[30] C. Figueroa, I. Vignon-Clementel, K.E. Jansen, T. Hughes, C. Taylor. A coupled momentum method for modeling blood flow in three-dimensional deformable arteries. *Comput. Methods Appl. Mech. Eng.* 195: 5685–5706, 2006.

[31] L. Formaggia, J.F. Gerbeau, F. Nobile, A. Quarteroni. On the coupling of 3D and 1D Navier-Stokes equations for flow problems in compliant vessels. *Comput. Methods Appl. Mech. Eng.*, 191 (6-7):561–582,2001.

[32] J. Gerbeau, M. Vidrascu. A quasi-Newton algorithm based on a reduced model for fluid-structure interactions problems in blood flows. *Math. Model. Numer. Anal.* 37 (4):631–648, 2003.

[33] R. Glowinski. Finite element methods for incompressible viscous flow, in: P.G.Ciarlet, J.-L.Lions (Eds), Handbook of numerical analysis, volume 9. North-Holland, Amsterdam, 2003.

[34] G. Guidoboni, R. Glowinski, N. Cavallini, and S. Čanić. Stable loosely-coupled-type algorithm for fluid-structure interaction in blood flow. *J. Comput. Phys.*, 228(18):6916–6937, 2009.

[35] P. Hansbo. Nitsches method for interface problems in computational mechanics. *GAMM-Mitt.*, 28(2):183–206, 2005.

[36] M. Heil. An efficient solver for the fully coupled solution of large-displacement fluid-structure interaction problems. *Comput. Methods Appl. Mech. Eng.* 193: 1–23, 2004.

[37] T. Hughes, W. Liu, and T. Zimmermann. Lagrangian-Eulerian finite element formulation for incompressible viscous flows. *Comput. Methods Appl. Mech. Eng.*, 29(3):329–349, 1981.

[38] I. Kukavica and A. Tuffaha. Solutions to a fluid-structure interaction free boundary problem. *DCDS-A*, 32(4):1355–1389, 2012.

[39] R. van Loon, P. Anderson, J. de Hart, F. Baaijens. A combined fictitious domain/adaptive meshing method for fluid-structure interaction in heart valves. *Int. J. Numer. Meth. Fluids.* 46:533–544, 2004.

[40] A. Hundertmark-Zaušková M. Lukáčová-Medvid'ová, G. Rusnáková. Kinematic splitting algorithm for fluidstructure interaction in hemodynamics. *Computer Methods in Appl. Mech. Engi.*, 2013; **265**:83-106

[41] H. Matthies, J. Steindorf. Numerical efficiency of different partitioned methods for fluid-structure interaction. *Z. Angew. Math. Mech.* 2 (80): 557–558, 2000.

[42] B. Muha and S. Čanić. Existence of a Weak Solution to a Nonlinear Fluid–Structure Interaction Problem Modeling the Flow of an Incompressible, Viscous Fluid in a Cylinder with Deformable Walls. *Arch. Ration. Mech. Anal.*, 207(3):919–968, 2013.

[43] B. Muha and S. Čanić. Existence of a weak solution to a fluid-multi-layered-structure interaction problem. *Journal of Differential Equations*, 256:658–706, 2014.

[44] B. Muha and S. Čanić. Existence of a weak solution to a fluid-structure interaction problem motivated by blood-artery-stent interaction. *In preparation*, 2014.

[45] B. Muha and S. Čanić. A Nonlinear, 3D Fluid-Structure Interaction Problem Driven by the Time-Dependent Dynamic Pressure Data: A Constructive Existence Proof. *Journal Communications in Information and Systems (CIS)*. Accepted 2013.

[46] C.M. Murea and S. Sy. A fast method for solving fluid-structure interaction problems numerically. *Int. J. Numer. Meth. Fl.*, 60(10):1149–1172, 2009.

[47] F. Nobile. Numerical approximation of fluid-structure interaction problems with application to haemodynamics. PhD Thesis, EPFL, Switzerland, 2001.

[48] F. Nobile, C. Vergara. An effective fluid-structure interaction formulation for vascular dynamics by generalized Robin conditions. *SIAM J. Sci. Comput.* 30 (2):731–763, 2008.

[49] C. Peskin. Numerical analysis of blood flow in the heart. *J. Comput. Phys.* 25: 220–252, 1977.

[50] C. Peskin, D.M. McQueen. A three-dimensional computational method for blood flow in the heart I. Immersed elastic fibers in a viscous incompressible fluid. *J. Comput. Phys.* 81(2): 372–405, 1989.

[51] A. Quaini. Algorithms for fluid-structure interaction problems arising in hemodynamics. PhD. Thesis, EPFL, Switzerland, 2009.

[52] A. Quaini and A Quarteroni. A semi-implicit approach for fluid-structure interaction based on an algebraic fractional step method. *Math. Models Methods Appl. Sci.*, 17(6):957–985, 2007.

[53] A. Quarteroni and A. Valli. *Domain decomposition methods for partial differential equations*. Numerical Mathematics and Scientific Computation. The Clarendon Press Oxford University Press, New York, 1999. Oxford Science Publications.

[54] A. Quarteroni, M. Tuveri, and A. Veneziani. Computational vascular fluid dynamics: problems, models and methods. *Computing and Visualization in Science*, 2:163–197, 2000. 10.1007/s007910050039.

[55] P.L. Tallec, J. Mouro. Fluid-structure interaction with large structural displacements. *Comput. Methods Appl. Mech. Eng.* 190: 3039–3067, 2001.

[56] S. Zhao, X. Xu, M. Collins. The numerical analysis of fluidsolid interactions for blood flow in arterial structures Part 2: development of coupled fluid-solid algorithms. *Proc. Instn. Mech. Eng. Part H* 212:241–252, 1998.

E-mail: canic@math.uh.edu, borism@math.hr and martina@math.uh.edu

Department of Mathematics, University of Houston, Houston, Texas 77204-3476